

Crystalline Structure of Poly(decamethylene sebacate). Repercussions on Lamellar Folding Surfaces

E. Armelin, A. Almontassir, L. Franco, and J. Puiggali*

Departament d'Enginyeria Química, Universitat Politècnica de Catalunya, Av. Diagonal 647, E-08028, Barcelona, Spain

Received November 2, 2001; Revised Manuscript Received January 2, 2002

ABSTRACT: The crystalline structure of poly(decamethylene sebacate) has been studied using transmission electron microscopy and X-ray diffraction. The polymer shows polymorphism, since fibers corresponding to both monoclinic and orthorhombic unit cells can be obtained depending on the draw and annealing conditions. The second structure can also be obtained from solution crystallization in polar solvents such as 1-hexanol. Molecular packing of this structure has been studied in detail taking into account both diffraction data and energy calculations. The unit cell contains two chain segments with a slightly distorted all-trans conformation and a chain setting angle similar to that reported for polyethylene. The two chain segments are shifted along the chain axis direction, as they are related by a glide plane n . Lamellar crystals are sectorized and show a regular folding surface structure. Two kinds of folds, constituted by methylene or by ester groups, can be deduced from the space group symmetry and the surface decoration.

Introduction

Most of the practical biodegradable polymers for biomedical applications are aliphatic polyesters.¹ Among them, those derived from hydroxyacids such as the naturally occurring poly(β -(*R*)-hydroxybutirate), commercialized by ICI, the polymers derived from glycolic acid and/or lactic acid, and polycaprolactone may be mentioned. However, only recently have polyesters prepared from the condensation of diols and dicarboxylic acids been regarded to be of great interest as degradable polymers due to the low molecular weights obtained in the first synthesis² and the lack of thermal and mechanical properties. These limitations have been overcome by the use of new catalysts and coupling reactions in such a way that Showa Highpolymer Co. has commercialized derivatives of adipic acid and/or succinic acid, and ethylene glycol and/or 1,4-butanediol (BIONOLLE) with high molecular weights, and good performance and processability.³

Structural studies on polyesters with the repeat unit $-\text{O}(\text{CH}_2)_n\text{OCO}(\text{CH}_2)_m\text{CO}-$ are scarce but reveal some interesting features. Thus, kink conformations can be found in polymers with a low number of methylene groups, such as 2-4, 2-6, 2-8, 4-4, 4-6, and 6-6 polyesters.⁴⁻⁹ In this way, quantum mechanical calculations on small diesters¹⁰ showed the tendency of methylene units to adopt gauche conformations when a short aliphatic segment is placed between two carbonyl groups. On the other hand, an extended conformation was postulated for polyesters with long polymethylene sequences.¹¹ In general, all the above referred polyesters crystallize according to monoclinic or orthorhombic unit cells,¹² the dimensions of the chain axis projected unit cell being similar to that reported for polyethylene¹³ when the polyester has an extended conformation. However, a structure refinement has not usually been undertaken, and consequently there is no information about either the setting orientation angle or the chain axis shift between the two chain segments that belong to the unit cell. Energy calculations¹⁴ suggest structures with an orientation of methylene segments similar to

that of polyethylene. Furthermore, a glide plane a has usually been postulated for relating the two molecules of the unit cell. Consequently, molecular chain segments were not shifted along the chain axis direction when they pack according to orthorhombic unit cells, and models were built by placing the ester groups of the different chains at the same level. It is only recently that structural studies carried out with poly(tetramethylene succinate)¹⁵ and poly(hexamethylene sebacate)¹⁶ demonstrated that the two molecular chains of the unit cell were related by a diagonal glide plane n , and therefore a significant shift between these molecules must be considered in all calculations. The main goal of this work is the study of polyester 12 10 in order to gather more the structural data for polyesters with long polymethylene sequences.

Experimental Section

Polyester 12 10 was synthesized from sebacic acid and an excess of 1,12-dodecanediol (molar ratio 2.2/1) by thermal polycondensation in a vacuum at 200 °C and using titanium butoxide as a catalyst (yield 75%). An intrinsic viscosity of 1.01 dL/g was measured in dichloroacetic acid at 25 °C. A Water Assoc. apparatus (model 510) equipped with a Maxima 820 computer program was used for GPC analysis. The polymer was dissolved and eluted in a chloroform/*o*-chlorophenol (90/10, v/v) mixture at a flow rate of 0.5 mL/min (injected volume 100 μ L, sample concentration 2.5 mg/mL). A set of two μ -Stirigel (Polymer Lab.) columns with a limited exclusion weight of 10⁴ and 10³ and a RI 410 (Water Assoc.) detector were used. Number- and weight-average molecular weights of 37 800 and 99 800, respectively, were estimated using polystyrene standards (Polysciences). These values demonstrated a high molecular weight, as had been manifested by the film- and fiber-forming characteristics of the polymer. Density of fibers was measured at 25 °C by the flotation method in mixtures of ethanol and CCl₄.

Isothermal crystallization was carried out in the 30–60 °C range from dilute solutions (0.01% w/v) in 1-hexanol. The crystals were recovered from mother liquor by centrifugation, repeatedly washed with 1-butanol, and deposited on carbon-coated grids, which were shadowed with Pt-carbon at an angle of 15° for bright field observations. Polymer decoration was

achieved by evaporating polyethylene onto the surface of single crystals, as described by Wittmann and Lotz.¹⁷ A Philips TECNAI 10 electron microscope was used and operated at 80 and 100 kV for bright field and electron diffraction modes, respectively. Selected area electron diffraction patterns were recorded on Kodak Tri-X films. The patterns were internally calibrated with gold ($d_{111} = 2.35 \text{ \AA}$).

X-ray diagrams were recorded under vacuum at room temperature, with calcite as a calibration standard. A modified Statton camera (W.R. Warhus, Wilmington, DE) with Ni-copper radiation of wavelength 1.542 \AA was used. Fibers were prepared from the melt and annealed under stress at $55 \text{ }^\circ\text{C}$. Mats of sedimented crystals were prepared by slow filtration on a glass filter of a crystal suspension in 1-butanol.

Structural modeling was carried out by using the software packages (diffraction and energy minimization) of the CERIUUS^{2.0} (Biosym/Molecular Simulations Inc.)¹⁸ and the Prediction of Crystal Structure of Polymers¹⁹ (PCSP) computer programs. Basically, in the energy minimization (CERIUUS^{2.0} and PCSP), the relative stability of the different arrangements for a given packing was evaluated when the azimuthal orientation of the molecules was varied. Energy contributions of both van der Waals and electrostatic interactions concerning closely spaced nonbonded atoms were taken into account. The values for potential constants were taken from Dreiding (CERIUUS^{2.0}) and Amber²⁰ (PCSP) force-field libraries, whereas the partial charges were explicitly derived from a representative small compound by using a well-established methodology.²¹ All the calculations were run on a Silicon Graphics Indigo workstation.

Results and Discussion

X-ray Diffraction Data. Fibers obtained directly from the melt state show an oriented X-ray diffraction pattern that corresponds to a mixture of two structures. Note the presence of meridional and off meridional spots in the first layer line of Figure 1a, which could only be interpreted as the $00l$ reflections of two different crystalline forms. The former is characterized by a cc^* angle close to 26° , which is in agreement with the values reported for other polyesters with a planar conformation and a monoclinic structure (23° and 25° for polyesters 6 10¹⁶ and 10 18¹¹, respectively). A pattern corresponding only to the second form could be obtained when the fiber was annealed under tension at $50 \text{ }^\circ\text{C}$ for 30 min (Figure 1b). All the observed sharp reflections could be indexed according to an orthorhombic lattice of $a = 4.88 \text{ \AA}$, $b = 7.44 \text{ \AA}$, and c (chain axis) $= 29.84 \text{ \AA}$. These parameters are in agreement with a practically all-trans conformation (a value of 29.92 \AA is expected for the standard bond distances and bond angles of methylene and ester groups) and a unit cell containing two chain segments. Thus, the calculated density of 1.13 g/cm^3 compares well with the experimental value of 1.09 g/cm^3 . Reflections summarized in Table 1 show only systematic absences for $0kl$ ($k + l$: odd). Therefore, only a diagonal glide plane n perpendicular to the a crystallographic axis could be deduced from the X-ray diffraction data.

The same structure is obtained when the polymer is isothermally crystallized from dilute solutions (0.01% w/v) in 1-hexanol. Thus, the X-ray diffraction patterns of mats of sedimented crystals show the 002 reflection at 14.9 \AA , a value higher than the observed one (13.4 \AA) for the nonorthorhombic lattice. The indicated patterns also show meridional reflections associated with different lamellar orders (Table 1 and Figure 2). The deduced lamellar thickness slightly increases with the crystallization temperature, as it had been previously reported for different polyesters.²² Thus, values of 100,

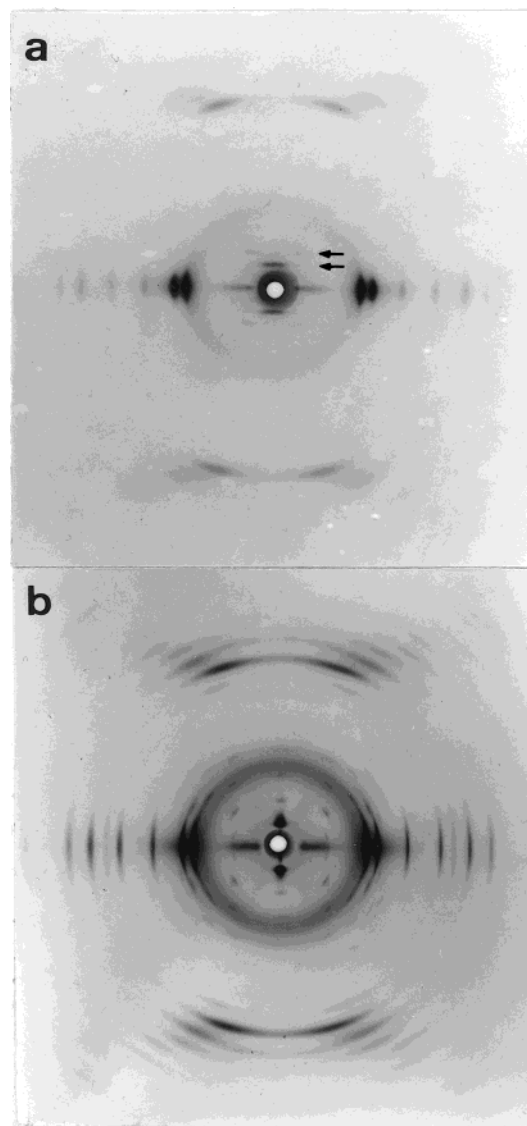


Figure 1. X-ray fiber diffraction patterns of polyester 12 10 corresponding to a mixture of two crystalline structures (a) and a pure orthorhombic lattice (b). First and second layer lines are indicated by arrows in (a).

104, and 112 \AA were obtained when crystallizations were conducted at 30, 40, and $50 \text{ }^\circ\text{C}$, respectively.

Electron Microscopy. Polyester 12 10 crystallizes from 1-hexanol solutions as large single crystals, whose lateral dimensions can reach $20\text{--}30 \text{ }\mu\text{m}$. Morphologies can be envisaged as both distorted hexagonal or lozenge truncated crystals. Small crystals show serrated front edges, but a curved lateral habit is more apparent when the dimensions are in the order of several microns. Rounded crystal boundaries have been observed for polyethylene crystallized at high temperature and have been explained in terms of a crystal growth that is not controlled by the surface nucleation.²³ Most of the crystals were in the form of spiral growths, but a few monolayer single crystals (Figure 3) could also be observed. The thicknesses of these crystals, measured from their platinum-carbon shadows on electron micrographs, were in the $100\text{--}110 \text{ \AA}$ range and consequently in agreement with the X-ray diffraction data.

Electron diffraction patterns show an mm symmetry and $hk0$ reflections up to 4 orders (Figure 4). No reflections from planes with $l \neq 0$ were detected, a fact

Table 1. Measured and Calculated X-ray Diffraction Spacings from Different Samples of the Orthorhombic Lattice of Polyester 12 10

index	d_{cal}^a	d_{meas}^b	
		fiber pattern	mat of crystals
1st lamellar order	112		
2nd lamellar order	56		56 vs M
3rd lamellar order	37.3		37.5 m M
4th lamellar order	28		28 vw M
5th lamellar order	22.4		20.5 m M
6th lamellar order	18.7		
002	14.9	15.0 vs M	14.9 s M
004	7.45	7.46 m M	
011	7.22	7.22 w off M	7.23 m E
013	5.95	6.00 m off M	6.05 m off M
006	4.97	4.93 m M	5.04 m M
015	4.65	4.60 m off M	4.65 m off M
102	4.64	4.61 m off M	4.68 m E
104	4.08	4.09 m off M	
110	4.08	4.08 vs E	4.08 vs E
113	3.77	3.76 m off M	
008	3.72	3.71 m M	
020	3.72	3.72 vs E	3.72 vs E
017	3.69	3.66 m off M	
022	3.61	3.58 m off M	
106	3.48	3.49 m off M	
024	3.33	3.28 m off M	
120	2.96	2.96 s E	2.96 s E
01,11	2.55	2.58 vw off M	
200	2.44	2.44 s E	2.44 s E
10,11	2.37	2.36 vw off M	
210	2.32	2.33 m E	
10,12	2.21	2.22 vs off M	2.23 vs M
130	2.21	2.20 s E	
11,12	2.12	2.10 s off M	2.13 m off M
02,12	2.07	2.03 m off M	
220	2.04	2.05 s E	
12,11	2.00	1.96 w off M	
040	1.86	1.84 w off M	
03,11	1.83	1.86 w off M	
230	1.74	1.74 vw E	

^a On the basis of an orthorhombic lattice with $a = 4.88 \text{ \AA}$, $b = 7.44 \text{ \AA}$, and $c = 29.8 \text{ \AA}$ and a crystal with a thickness of 112 \AA .

^b Abbreviations denote relative intensities or orientation: vs, very strong; s, strong; m, medium; w, weak; vw, very weak; M, meridional; E, equatorial and off M, off meridional.

that indicates a perpendicular orientation of molecular chains to the basal plane of the single crystals. All the observed reflections could be well-indexed with the a and b parameters previously reported, 110 (4.08 \AA) and 020 (3.72 \AA) being the most intense ones. No systematic absences for $hk0$ ($h + k$ odd) could be detected, and thereby a C-centered unit cell could be rejected from the electron diffraction data. Correlation of the bright-field micrographs and the electron diffraction patterns indicated that the growth faces of the single crystals correspond to the $\{110\}$ and $\{010\}$ planes.

Crystals were sensitive to crystallization temperature. Thus, growth along the $\{010\}$ faces becomes enhanced with temperature as is well-known for polyethylene.^{24,25} (In this case, the orthorhombic unit cell was defined with the a and b parameters interchanged, and consequently the $\{100\}$ face was the equivalent one.) Spiral growths are more frequently observed in the polyester crystallized at higher temperature. In the same way, the growth faces become worse defined and the thickness of the crystals increased.

The fold-surface structure of polyester 12 10 was investigated by the surface decoration method developed by Wittmann et al.¹⁷ Figure 5 shows an example of decoration with polyethylene, which was deposited from

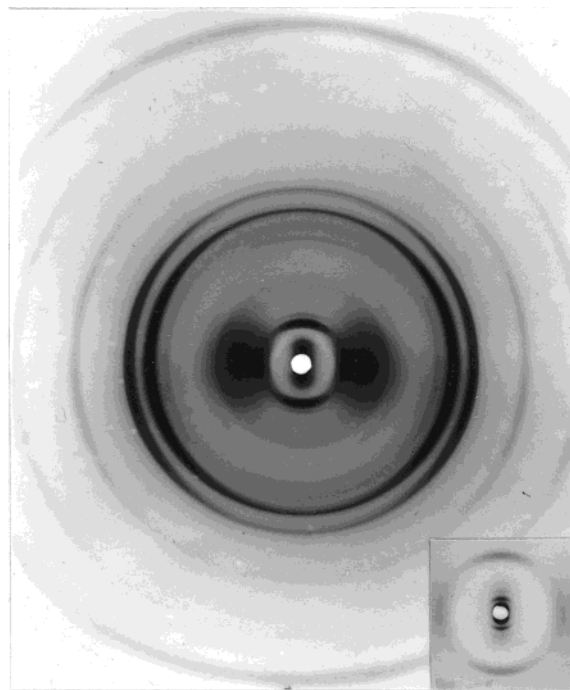


Figure 2. Wide-angle X-ray diffraction pattern from a mat of sedimented crystals. Meridional reflections related to the lamellar thickness are present in the low-angle pattern (inset). The second lamellar order at 56 \AA is clearly visible for the crystals obtained at $50 \text{ }^\circ\text{C}$.

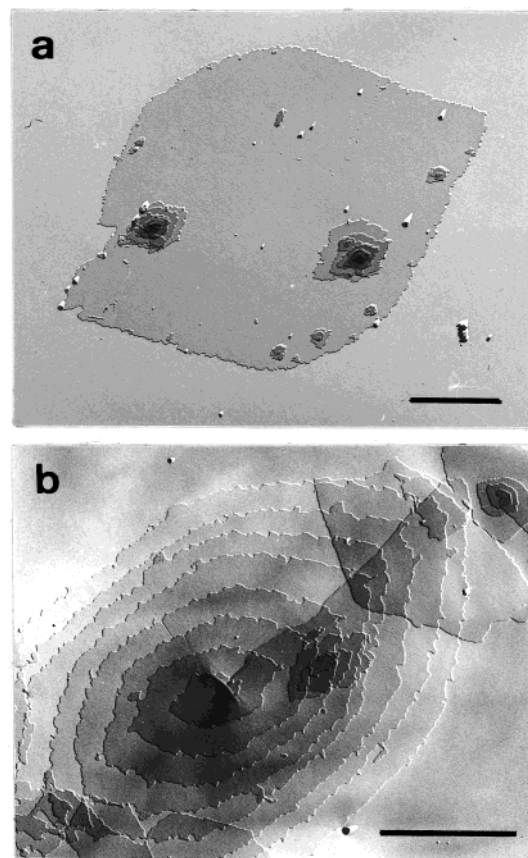


Figure 3. Transmission electron micrographs of lamellar crystals of polyester 12 10 grown in 1-hexanol. Single crystals shadowed with Pt/C show a regular thickness close to 10 nm and irregular front edges. Monolayer single-crystal grown at $30 \text{ }^\circ\text{C}$ (a) and crystals formed through spiral growth on the mother crystal at $50 \text{ }^\circ\text{C}$ (b). Scale bars $2.5 \text{ }\mu\text{m}$.

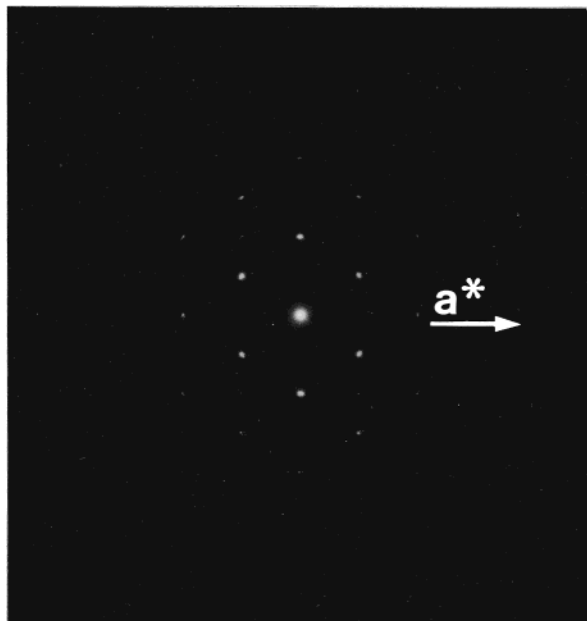


Figure 4. Selected area electron diffraction pattern of a crystal of polyester 12 10 obtained by crystallization in 1-hexanol at 30 °C. The pattern was obtained with the electron beam perpendicular to the basal plane of the lamella and consequently parallel to both c and c^* axes due to the orthorhombic lattice. a^* always appears to be oriented along the large dimension of the crystals. Some weak $h00$ and $0k0$ reflections (h or k odd) could be detected despite the fact that they would correspond to systematic absences. Dynamic scattering effects would probably be the main explanation.

its vapor phase. Note that the rodlike crystals of polyethylene are oriented in some regular fashion in each sector of the polyester single crystals. Basically, the long axis of these crystals is disposed normal to the growth face of each sector, though the $\{110\}$ sectors appear to be more regular than the $\{010\}$ ones. Accordingly, it may be supposed that molecular chains are preferentially folded along the $\{110\}$ and $\{100\}$ directions in the $\{110\}$ and $\{010\}$ sectors, respectively. Note that these directions correspond to that where neighboring chains are closer.

Structural Modeling. The expected molecular symmetry for an extended conformation is $2/m$ with inversion centers in the middle of both diacid and diol moieties and with a mirror plane which contains all the methylene carbons. Only the centers of symmetry can be preserved in the space group when the angle between the plane constituted by the methylene carbons and the ac crystallographic plane is different from 0 or 90°. We will use the indicated angle to define the setting orientation angle of a molecular chain. Note that the mirror plane symmetry will also be lost for a distorted trans conformation, that is, when the conformation deviates from the planar one. This reduced molecular symmetry, the detected systematic absences, and the two chain segments containing unit cell strongly suggest that the symmetry corresponds to the monoclinic space group $P2_1/n11$. Note that it is not possible to find the symmetry elements required for an orthorhombic space group, which could justify the experimental lattice with angles equal to 90°.

In a first approximation, the X-ray fiber diffraction patterns were simulated with the Cerius^{2.0} program by considering the indicated monoclinic space group and a planar conformation. Thus, only the setting angle was

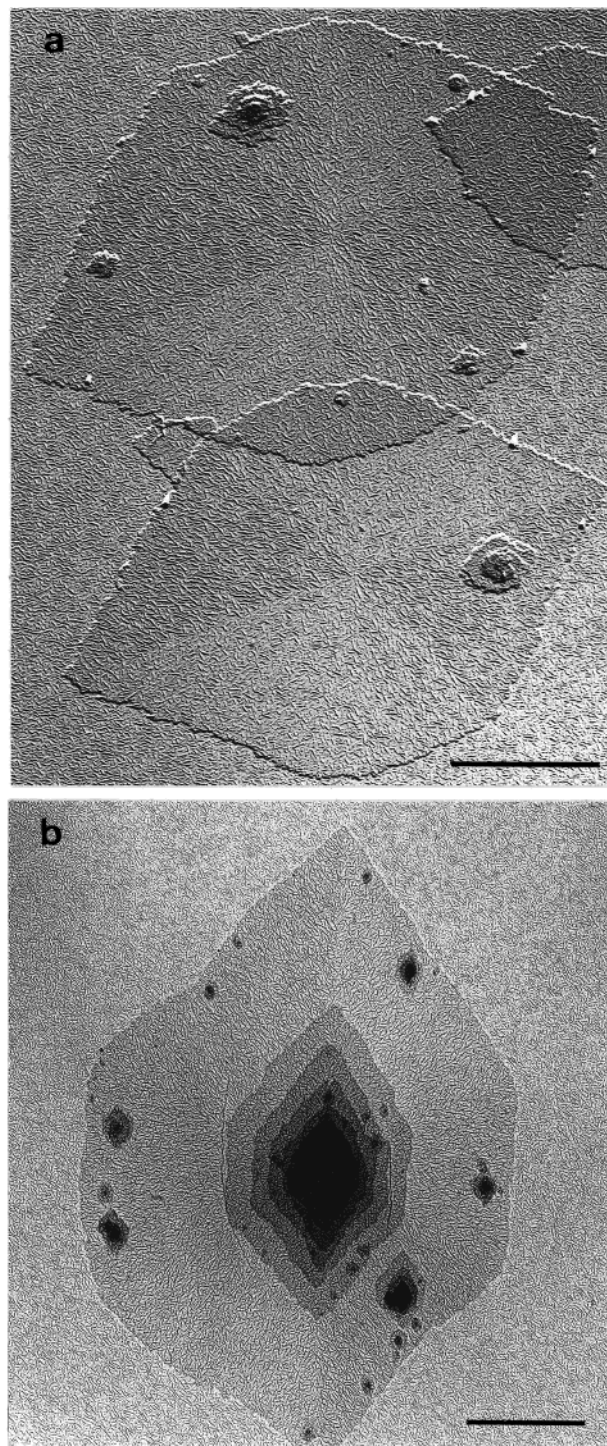


Figure 5. Polyethylene decoration of polyester 12 10 single crystals demonstrated their sectorization and the occurrence of regular fold surfaces. (a) Decorated crystals were shadowed with Pt/C at an angle of 15°. Note that two $\{110\}$ sectors are well-defined. Scale bar: 2.5 μm . (b) Decorated crystals shadowed as explained above but rotating the grid. In this case, all sectors can be visualized, though less defined. Scale bar: 5 μm .

regularly varied in steps of 5°. The best agreement was obtained when this angle reached the value of 45° (Figure 6a). Observe that the intensity of the equatorial reflections is well-simulated, but a major discrepancy with the experimental pattern is observed for some hkl reflections (i.e., compare the relative intensities between the 011 and 013 reflections in both simulated and experimental patterns). However, a significant improve-

Table 2. Relative Packing Energies^a (kcal/mol unit cell) and Setting Angles (deg) for the Polyester 12 10 According to Different Space Groups and Conformations

space group	trans conformation				distorted trans conformation		
	ΔE_{ele}^b	ΔE_{vdW}^c	ΔE_{T}^d	setting angle ^e	ΔE_{ele}^b	ΔE_{vdW}^c	ΔE_{T}^d
<i>P2</i> ₁ / <i>n</i> 11	2.1	5.2	6.4	33	0	5.4	1.9
<i>P2</i> ₁ / <i>b</i> 11	0	2.8	1.9	38	3.5	0	0
<i>P12</i> ₁ / <i>n</i> 1	0.2	2.8	2.1	21	2.4	5.4	4.3
<i>P12</i> ₁ / <i>a</i> 1	0.9	0	0	29	7.9	9.6	14

^a Only data calculated with the CERIUSt^{2.0} program are provided. ^b Electrostatic contribution. ^c van der Waals contribution. ^d Total relative energy. ^e Defined as the angle between the plane constituted by the methylene carbons and the *a* crystallographic axis.

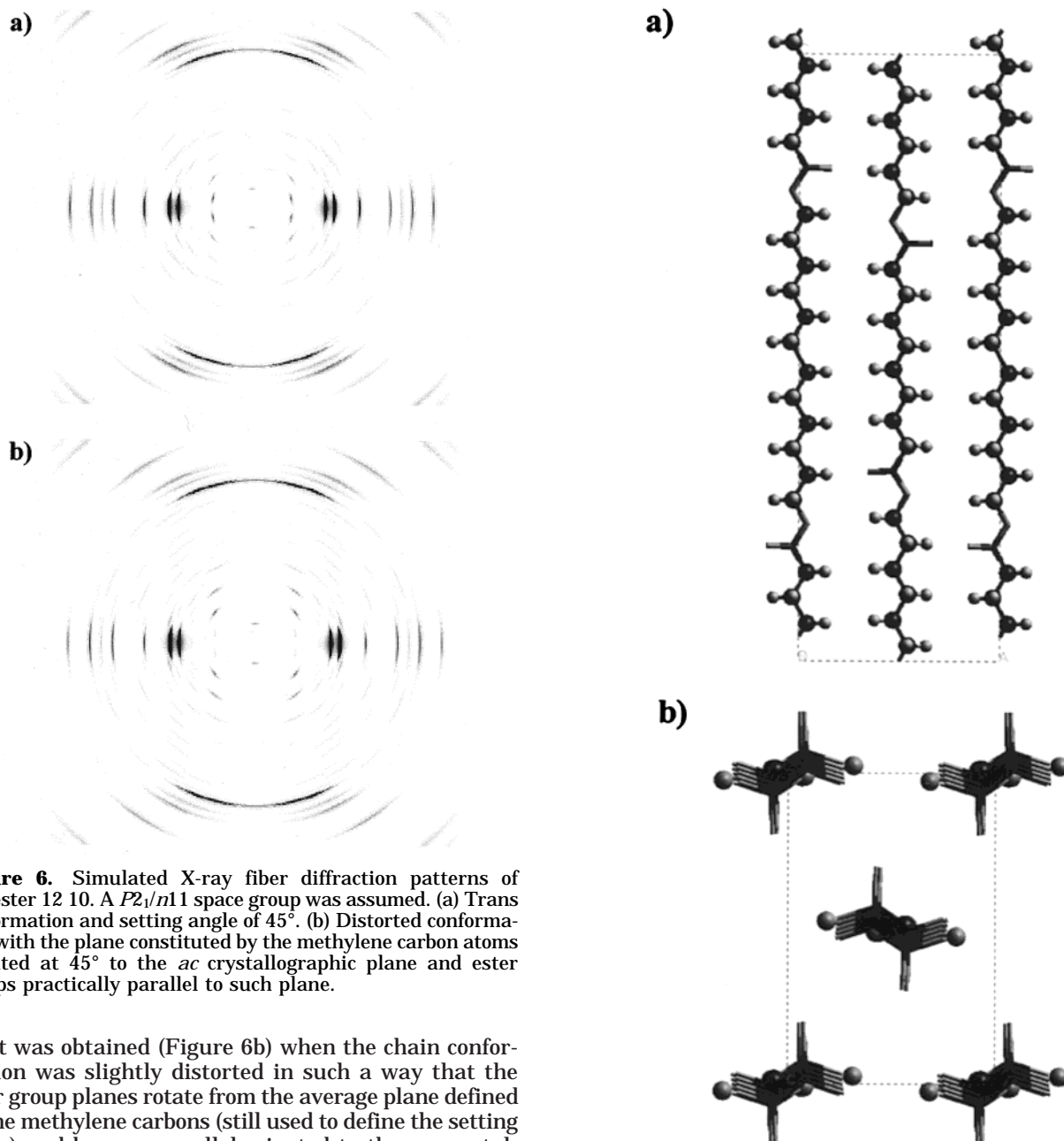


Figure 6. Simulated X-ray fiber diffraction patterns of polyester 12 10. A *P2*₁/*n*11 space group was assumed. (a) Trans conformation and setting angle of 45°. (b) Distorted conformation with the plane constituted by the methylene carbon atoms oriented at 45° to the *ac* crystallographic plane and ester groups practically parallel to such plane.

ment was obtained (Figure 6b) when the chain conformation was slightly distorted in such a way that the ester group planes rotate from the average plane defined by the methylene carbons (still used to define the setting angle) and become parallel-oriented to the *ac* crystallographic plane. This modification involved only the CH₂–CH₂–O–CO (φ) and O–CO–CH₂–CH₂ (ψ) torsional angles by keeping the relationship $\varphi = -\psi = 150^\circ$. A chain axis parameter of 29.8 Å was estimated for this conformation, in agreement with the experimental data.

Packing energy calculations were also carried out in order to obtain the optimum setting angle. For the sake of completeness, we considered four packing possibilities. These correspond to the *P2*₁/*n*11, *P2*₁/*b*11, *P12*₁/*n*1,

Figure 7. Views of the proposed polyester 12 10 in a distorted all-trans conformation: (a) View parallel to the *b*-axis direction. To show the packing more clearly, the *a* parameter was doubled. In the same way, a ball-and-stick representation was used for methylene groups, whereas cylinders were used for the ester groups. (b) View parallel to the *c*-axis direction. In this case, the scale was doubled and a different representation was used for methylene (cylinders) and ester groups (ball-and-stick). Color code: hydrogen and oxygen, gray; carbon, black.

*n*1, and *P12*₁/*a*1 monoclinic space groups. Note that in all these cases the center of symmetry is kept, and the

two chain segments of the unit cell are related by a 2-fold screw axis. In each case, the energy was minimized by varying only the setting angle and considering both van der Waals and electrostatic interactions. For comparison purposes, we used two different force fields, Dreiding and Amber, which are implemented in the CERIU^{2.0} and PCSP programs. Similar results were obtained with the two indicated programs. Particularly, the same values of the setting angles were found in the minimized packing of each structure. Slight but not significant differences were found between the relative packing energy stabilities (van der Waals, electrostatic, and total). The results reported in Table 2 (only for the CERIU^{2.0} calculations) are very meaningful. Thus, the $P2_1/n11$ space group is the most energetically disfavored structure, in clear disagreement with the explained experimental evidence. Notice that both the van der Waals and Coulombic interactions have the highest relative energies. We interpret this fact as a clear sign of the distortion of the planar molecular conformation. In this sense, when calculations were done by considering the conformation defined by $\varphi = -\psi = 150^\circ$, a dramatic change in the packing energy values was found (Table 2). $P2_1/n11$ was the most favored structure, taking into account only the electrostatic interactions. The structure was minimized with a setting angle of 38° and hence close to the X-ray deductions. However, $P2_1/b11$ had the absolute minimum packing energy when all interactions were considered. In this sense, we must indicate the simplicity of our model, which only considered variations in the φ and ψ torsional angles.

Projections of the minimized packing for the $P2_1/n11$ space group are shown in Figure 7. Note that neighboring chains in the 110 plane have a shift of $c/2$. This is an interesting feature that influences the regular fold surface of the $\{110\}$ sectors. Thus, ester groups must be involved in these folds; otherwise, a hydroxyacid unit will appear in the sequence of the folded chain due to the reversal of the O–CO sequence. Note also that, for similar considerations, the folds in the $\{010\}$ sectors must take place through methylene groups. These considerations have also been recently described for the monoclinic lattice of polyester 6 10¹⁶.

Conclusions

The diffraction data from fibers and single crystals of polyester 12 10 suggest a preferred structure that is characterized by an orthorhombic lattice and a unit cell containing two chain segments. Single crystals are

sectorized and have some regular folding surface structure. Thus, molecular chains fold predominantly along the $\{110\}$ and $\{100\}$ crystallographic directions in the $\{110\}$ and $\{010\}$ sectors, respectively.

Chain segments of the unit cell are related by a diagonal glide plane and are consequently shifted by $c/2$. This packing symmetry has important repercussions on the lamellar folding surface. Folds constituted by methylene groups have to occur along the $\{100\}$ direction, where chain segments are not shifted, whereas ester groups must be involved along the $\{110\}$ direction, where the indicated $c/2$ shift exists.

Acknowledgment. This research work has been supported by CICYT (MAT2000-0995).

References and Notes

- (1) Huang, S. J. In *Encyclopedia of Polymer Science and Engineering*; Wiley-Interscience: New York, 1985; Vol. 2, p 20.
- (2) Carothers, W. H. *Chem. Rev.* **1931**, *8*, 353.
- (3) Fujimaki, T. *Polym. Degrad. Stab.* **1997**, *30*, 7403.
- (4) Ueda, A. S.; Chatani, Y.; Tadokoro, H. *Polym. J.* **1991**, *2*, 387.
- (5) Turner-Jones, A.; Bunn, C. W. *Acta Crystallogr.* **1962**, *15*, 105.
- (6) Chatani, Y.; Hasegawa, R.; Tadokoro, H. In *Meeting of the Society of Polymer Science (Japan)*, 1971; p 420.
- (7) Minke, R.; Blacwell, J. *J. Macromol. Sci., Phys.* **1979**, *B16*, 407.
- (8) Minke, R.; Blacwell, J. *J. Macromol. Sci., Phys.* **1980**, *B18*, 233.
- (9) Aylwin, P. A.; Boyd, R. H. *Polymer* **1984**, *25*, 323.
- (10) Alemán, C.; Puiggali, J. *J. Org. Chem.* **1997**, *62*, 3076.
- (11) Kanamoto, T.; Tanaka, K. *J. Polym. Sci., Part A-2* **1971**, *9*, 2043.
- (12) Brandrup, J.; Immergut, E. H. In *Polymer Handbook*; Wiley-Interscience: New York, 1989.
- (13) Swan, P. R. *J. Polym. Sci.* **1962**, *56*, 403.
- (14) Liau, W. B.; Boyd, R. H. *Macromolecules* **1990**, *23*, 1531.
- (15) Ichikawa, Y.; Kondo, H.; Igarashi, Y.; Noguchi, K.; Okuyama, K.; Washiyama, J. *Polymer* **2000**, *41*, 4719.
- (16) Armelin, E.; Casas, M. T.; Puiggali, J. *Polymer* **2001**, *42*, 5695.
- (17) Wittmann, J. C.; Lotz, B. *J. Polym. Sci., Part B: Polym. Phys.* **1985**, *23*, 205.
- (18) Cerius² 2.0, Molecular Simulations Inc., Burlington, MA.
- (19) León, S.; Navas, J. J.; Alemán, C. *Polymer* **1999**, *40*, 7351.
- (20) Weiner, S. J.; Kodman, P. A.; Nguyen, D. T.; Cabe, D. A. *J. Comput. Chem.* **1986**, *7*, 230.
- (21) Alemán, C.; Luque, F. J.; Orozco, M. *J. Comput.-Aided Mol. Des.* **1993**, *7*, 721.
- (22) Girolamo, M.; Keller, A.; Stejny, J. *Makromol. Chem.* **1975**, *176*, 1489.
- (23) Sadler, D. M. *Polymer* **1983**, *24*, 1401.
- (24) Hoffman, J. D.; Miller, R. I. *Macromolecules* **1989**, *22*, 3038.
- (25) Tanzawa, Y.; Toda, A. *Polymer* **1996**, *37*, 1621.

MA011918T